

Computer-Aided Design of RF Structures

D.T. Tran, A. Cailleaux and G. Berthevas
Thomson-CSF Electron Tube Division
BP 305 - 92102 Boulogne-Billancourt Cedex, France

Summary

Recently a method has been developed to calculate RF-structures without cylindrical symmetry. Geometries considered consisted of a repetition of two cylindrical segments, each characterized by a section of any shape, for which eigenmodes are calculated from a two-dimensional code (HELMOT-2D). They were assumed to have translational symmetry. In this paper, we present again this method but generalized to the case of helical symmetry, that is, segments can be rotated from each other by any constant angle (POSTEL-Code), along with a three-dimensional treatment (HELMOT-3D Code) which begins to give encouraging results. Theoretical results and measurements are compared on two RF-structures chosen for illustration.

Introduction

In the design of RF-structures for microwave tubes and linear accelerators, the knowledge of the whole pass-band and sometimes of the neighbouring bands is of great importance. When a new design has to be found to meet new performance specifications, systematic investigation by experimental modeling appears to be imprecise, time consuming, and very expensive. For this reason, computer-aided investigation tools are being developed; firstly, to help find the adequate structure, and secondly to refine it. The two codes presented here, namely POSTEL and HELMOT-3D, have been formulated by Thomson-CSF in an attempt to fulfill these needs.

Two Segment RF-Structure with Helical Symmetry

Recently, a theory has been developed and applied to RF-structures without axial symmetry (1). The structure treated was a two-segment system, assumed to have translational symmetry, that is, the whole structure can be generated by translation of a single period. In this section, this theory is generalized to the case of helical symmetry, that is, segments can be rotated from each other by any constant angle. Such geometries would cover a number of practical cases, some samples of which are illustrated in Figure 1.

Field Expressions

Basically, the theory is developed following the well-known field matching method presented in a previous paper (1) making use of a coupled eigenmode formalism, wherein the TE and TM-components are represented by the longitudinal components of magnetic and electric fields:

$$H_z = \sum_n [X_n F_2(\alpha_n z) - j Y_n F_1(\alpha_n z)] \psi_n(r), \quad (1)$$

$$E_z = \sum_n [W_n F_2(\beta_n z) - j S_n F_1(\beta_n z)] \varphi_n(r) \quad (2)$$

$\psi_n(r)$ and $\varphi_n(r)$ are the scalar parts of the TE and TM-Hertz vectors, respectively, which are solved for each of the two cylindrical segments with the help of the HELMOT-2D code (2). α_n and β_n are the corresponding propagation constants, and F_1 and F_2 are the odd and even longitudinal eigenfunctions chosen such that they have values of ± 1 at the extremities of each segment. X and Y , on one hand, and W and S , on the other hand, are, respectively, the real and complex parts of the modal components of the current vector $\vec{J}(X_1, Y_1; \dots; X_n, Y_n)$ and the voltage vector $\vec{\psi}(W_1, S_1; \dots; W_n, S_n)$. We use the following 2×2 rotation matrices:

$$\begin{aligned} \tilde{T}_0(\alpha_m z) &= \begin{pmatrix} F_2(\alpha_m z) & 0 \\ 0 & F_1(\alpha_m z) \end{pmatrix} \\ P &= \begin{pmatrix} 1 & 0 \\ 0 & -1 \end{pmatrix}, \quad R = \begin{pmatrix} 0 & 1 \\ 1 & 0 \end{pmatrix}, \quad S = \begin{pmatrix} 0 & -1 \\ 1 & 0 \end{pmatrix} \text{ and} \\ \phi &= \begin{pmatrix} \cos \beta L & -\sin \beta L \\ \sin \beta L & \cos \beta L \end{pmatrix}, \end{aligned} \quad (3)$$

where βL is a half period phase shift. The 0 indices in \tilde{T}_0 signifies a zero-angle rotation (the case of translational symmetry) and similarly, in the following, the Θ subscript in \tilde{T}_Θ , for a rotation of angle Θ .

Using this notation, the z-components of the magnetic and electric field can be written in the following closed forms:

$$H_z(z, r) = \tilde{T}(\alpha z) P \tilde{J} \psi(r), \quad (4)$$

$$E_z(z, r) = \tilde{T}(\beta z) P \vartheta \varphi(r), \quad (5)$$

from which can be derived the other transverse components.

Floquet's Theorem and the Field Matching Principle

With field components written in the complex form of Eq (4) and Eq (5), it can be verified that the application of Floquet's theorem consists in multiplying field expression by ϕ^{-2} when one moves along the structure by one period $2L$, as shown in Table 1.

Table 1

Segment 2-2L	Segment 1	Segment 2	Segment 1+2L
ϕE_2	E_1	$\phi^{-1} E_2$	$\phi^{-2} E_1$
$-a_1$	a_1	$-a_2$	a_2

In Table 1, the field expression is written in the coordinate system of the corresponding segment and the origin of ϕ is taken at the center of segment 1. It can be noticed that, due to symmetry, a center to center translation corresponds to multiplying the field by ϕ , the half period phase shift matrix. The field matching principle imposes the condition of the continuity of the electric field at the segment boundaries, which can be written as:

$$E_1(a_1) = \phi^{-1} E_2(-a_2), \quad (6)$$

$$E_1(-a_1) = \phi E_2(a_2), \quad (7)$$

and similarly for H . Eq (6) and Eq (7) are exact field matching equations, however, it is known that only transverse components need be taken into account (3). Furthermore, due to the orthogonality of ψ and φ , Eq (6) and (7) can be written in simple integral forms by using coupling coefficients (1, 2) defined as:

$$\begin{aligned} h_{mn} &= \int_{S_1} \psi_{2m} \psi_{1n} dS, \quad e_{mn} = \int_{S_1} \varphi_{2m} \varphi_{1n} dS \quad \text{and} \\ e h_{mn} &= \int_{C_1} \varphi_{2m} \frac{d\psi_{1n}}{dC} dC, \end{aligned} \quad (8)$$

where indices 1 and 2 indicate the segment number.

Helical Symmetry

To better visualize the transformation to be applied to \tilde{T}_0 to yield \tilde{T}_Θ , let us consider the particular case of $\Theta = \pi$ and assume segment 2 such that it coincides with itself after a π -rotation (for example, a circular shape or square shape). It is assumed also that the radial coordinate system in segment 1 will perform the same rotation, i.e., field expressions in segment 1 remain unchanged by this rotation. For segment 2, two cases are to be considered. If the field pattern of eigenmode number n is antisymmetric with respect to the symmetry plane of the structure, i.e., its sign remains unchan-

ged by the π -rotation of the coordinate system, then $F_n = F_{0n}$. If, on the contrary, the field pattern is symmetric, the oddfunction F_{1n} has to be replaced by the even function $-F_{2n}$ (and vice versa) in order to take the sign change into account. This gives :

$$\tilde{\gamma}_{0n} = \begin{pmatrix} F_{2n} & 0 \\ 0 & F_{1n} \end{pmatrix} \Rightarrow \tilde{\gamma}_{\pi n} = - \begin{pmatrix} F_{1n} & 0 \\ 0 & F_{2n} \end{pmatrix} \quad (9)$$

or : $\tilde{\gamma}_{\pi n} = S \tilde{\gamma}_{0n} S$ (10)

where $\tilde{\gamma}$ is the transposed of $\tilde{\gamma}$. In observing that S is just a $\pi/2$ -rotation matrix, the generalization of Eq (10) to a general helical case is straightforward and yields :

$$\tilde{\gamma}_{\theta n} = \Theta^{1/2} \tilde{\gamma}_{0n} \Theta^{1/2} \quad (11)$$

where Θ is the rotation matrix of angle Θ . In particular for $\Theta = \pi/2$, one has :

$$\tilde{\gamma}_{\pi/2} = \frac{1}{\sqrt{2}} \begin{pmatrix} 1 & -1 \\ 1 & 1 \end{pmatrix} \begin{pmatrix} F_2 & 0 \\ 0 & F_1 \end{pmatrix} \frac{1}{\sqrt{2}} \begin{pmatrix} 1 & -1 \\ 1 & 1 \end{pmatrix} \quad (12)$$

Dispersion Equation

From Eq (4) and Eq (5), using the field-matching as expressed in Eq (6) and Eq (7), one obtains the following continuity equations for the transverse fields :

$$f(E) \equiv E_{t1}(a_1) + Q E_{t2}(a_2) = 0, \quad (13)$$

$$f(H) \equiv H_{t1}(a_1) + Q H_{t2}(a_2) = 0, \quad (14)$$

where the form of Q depends on the rotation angle and the symmetry of the field pattern in segment 2. To obtain the dispersion equation, Eq (13) and Eq (14) are replaced by the following integral forms :

$$\int_{S_2} \vec{k} \times \nabla \psi_{2n} \cdot f(E) dS = 0, \quad (15)$$

$$\int_{S_2} \nabla \varphi_{2n} \cdot f(E) dS = 0, \quad (16)$$

$$\int_{S_1} \vec{k} \times \nabla \psi_{1n} \cdot f(H) dS = 0, \quad (17)$$

$$\int_{S_1} \nabla \psi_{1n} \cdot f(H) dS = 0, \text{ for all } n. \quad (18)$$

Finally, by using the orthogonality property of ψ_n and φ_n , one obtains the following dispersion equation :

$$\begin{bmatrix} h & -\phi P & 0 & 0 \\ 0 & 0 & -\phi P & \bar{e} \\ \omega \mu_0 \frac{eh}{\mu_1^2} R & 0 & \nu_2^2 e \frac{1}{\mu_1^2} T_1(\beta_1 a_1) & Q K_2(\beta_2 a_2) \\ T_1(\alpha_1 a_1) & \mu_1^2 R \frac{1}{\mu_2^2} Q K_2(\alpha_2 a_2) & 0 & -\epsilon_0 \omega \frac{eh}{\mu_2^2} \phi^{-1} S \end{bmatrix} \begin{bmatrix} J_1 \\ J_2 \\ \phi_1 \\ \phi_2 \end{bmatrix} = 0 \quad (19)$$

where h, e, and eh represent infinite coupling matrices with elements of the form :

$$(h)_{ij} = h_{ij} \begin{pmatrix} 1 & 0 \\ 0 & 1 \end{pmatrix} \dots \quad (20)$$

$\nu^2, 1/\nu^2, \mu^2, 1/\mu^2$ are diagonal matrices, such as :

$$\nu_2^2 = \text{diag} \left\{ \nu_{2n}^2 \begin{pmatrix} 1 & 0 \\ 0 & 1 \end{pmatrix} \right\}, 1/\nu_2^2 = \text{diag} \left\{ 1/\nu_{2n}^2 \begin{pmatrix} 1 & 0 \\ 0 & 1 \end{pmatrix} \right\} \dots$$

where : $\mu_{2n}^2 = [(\omega/c)^2 - \alpha_{2n}^2]$, $\nu_{2n}^2 = [(\omega/c)^2 - \beta_{2n}^2]$, (21)

the indices 1 or 2 designating the segment. The coupling coefficients and the eigenvalues $\mu^2 n$ and $\nu^2 n$ are calculated from the finite element HELMOT-2D code. The Q and K-matrices have different forms, depending on the rotation angle and the field parity with respect to the symmetry plane. Let us consider three particular cases.

In the case of an aligned structure, Q and K are diagonal matrices of elements of the same type :

$$Q_{0n} = \phi^{-1} P; \quad (22)$$

$$K_{02n}(\alpha_{2n} a_2) = \alpha_{2n} \begin{pmatrix} \tan \alpha_{2n} a_2 & 0 \\ 0 & 1/\tan \alpha_{2n} a_2 \end{pmatrix} \quad (23)$$

In the case of an alternated structure, Q_n and K_n will have the form of Q_{0n} and K_{02n} if the corresponding eigemode has an antisymmetric field pattern, i.e., coinciding with itself with the same sign in a π -rotation. Otherwise Q_n and K_n take the forms :

$$Q_{\pi n} = -\phi^{-1} P \quad (24)$$

$$K_{\pi 2n}(\alpha_{2n} a_2) = \alpha_{2n} \begin{pmatrix} 1/\tan \alpha_{2n} a_2 & 0 \\ 0 & \tan \alpha_{2n} a_2 \end{pmatrix} \quad (25)$$

In the case of a crossed structure ($\Theta = \pi/2$), Q_n and K_n can take three different forms : Q_{0n} and K_{02n} for anti-symmetric field, $Q_{\pi n}$ and $K_{\pi 2n}$ for symmetric field or the following forms :

$$Q_{\pi/2 n} = \phi^{-1} R \quad (26)$$

$$K_{\pi/2 2n}(\alpha_{2n} a_2) = \frac{\alpha_{2n}}{\sin 2\alpha_{2n} a_2} \begin{pmatrix} 1 & -\cos 2\alpha_{2n} a_2 \\ -\cos 2\alpha_{2n} a_2 & 1 \end{pmatrix} \quad (27)$$

if field pattern is neither symmetric nor antisymmetric with respect to a $\pi/2$ -rotation but is symmetric with respect to a π -rotation.

Eq (19) is solved by the POSTEL code. For illustration, we consider a coupled-cavity structure. Field patterns of the 5 first TE-modes and the 4 first TM-modes of the coupling segment are given in Figure 2. Figure 3 and Figure 4 show the dispersion curves, calculated and measured, of an aligned and an alternated structure.

One can see that the precision of the calculation is sufficiently good to be used for a first investigation prior to a more precise design which may need a three dimensional or an experimental modeling with a more realistic shape.

The Three Dimensional Problem

In order to deal with geometries without symmetry, the HELMOT-3D code has been developed to solve the three dimensional problem. It is derived from the finite element HELMOT-2D code developed previously to solve the Helmholtz equation in the two dimensional case. The finite element method has been largely treated in the literature. We would just like to indicate that the two dimensional problem differs from a three dimensional one mainly in that, in the 2-D case, the zero divergence condition is satisfied by the appropriate choice of field vector and the Neuman condition is automatically taken into account in the finite element method itself. In the three dimension problem, on the contrary, though the first condition is theoretically insured it occurs sometimes that the discretization introduces spurious solutions with nonzero divergence. The cause is not exactly known but it appears that the choice of a zero divergence trial function may help.

The code was first tested on cylindrical cavities. The application of the code to cavities of realistic shape is in progress. The example given here corresponds to a klystron cavity with a rectangular envelope and a conic drift-tube which can be off-centered, as shown in Fig. 5. The side of the rectangular envelope for which the drift-tube is centered is 48 mm wide and the other side is measured by (A + B). The drift-tube is 24 mm ϕ_{ax} and 16 mm ϕ_{in} and 14,1 mm long. The first result on the lowest mode (shown in Table 3) is encouraging. In the second column, an improvement of the precision has been obtained by increasing the number of elements.

Table 2

A (mm)	18	18	30
B (mm)	18	18	24
Points (number)	1456	1546	1546
Elements (number)	260	276	276
Theory (MHz)	3206	3190	2705
Measured (MHz)	3175	3175	2690

Conclusion

The POSTEL code is currently used to shape RF-structures from given dispersion characteristics. As for HELMOT-3D, further work has to be undertaken in order to use computer memory and time more efficiently, and also to increase our understanding of the spurious solutions encountered in the investigation of higher order modes.

References

1. D.T. TRAN, IEEE NS-30 4, p 3636 (1983 Part. Accel. Conf.)
2. HELMOT-2D, a Finite Element Code of Thomson-CSF, DTE, unpublished

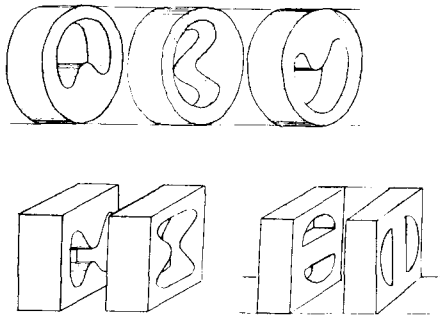


Figure 1 - Examples of two segment RF-structures

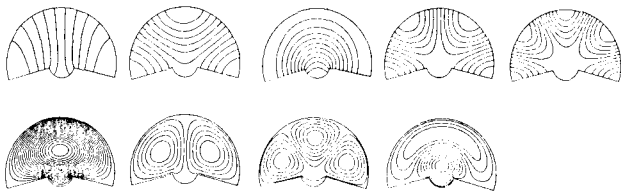


Figure 2 - Field patterns in coupling segment obtained from HELMOT-2D Code

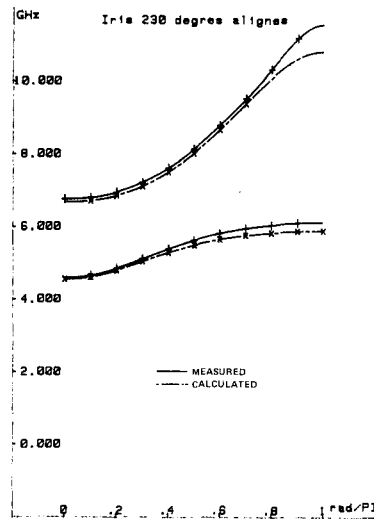


Figure 3 - Measured and calculated dispersion curves with aligned coupling segments

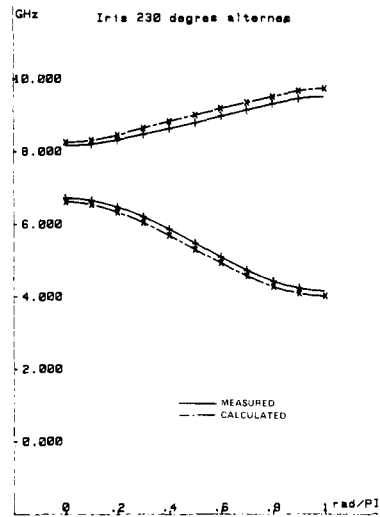


Figure 4 - Measured and calculated dispersion curves with alternated coupling segments

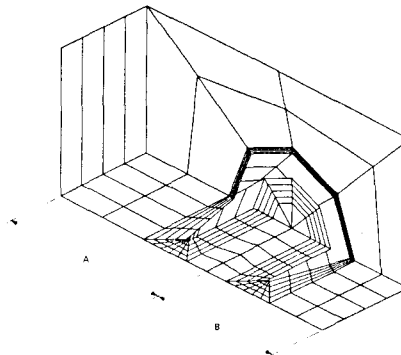


Figure 5 - Klystron (half-) cavity treated by HELMOT-3D Code